

SFGA: Similarity-Constrained Fusion Learning for Unsupervised Anomaly Detection in Multiplex Graphs

Huiliang Zhai^{1,2*}, Xiangyi Teng^{2*†}, Jing Liu^{1,2}

¹School of Artificial Intelligence, Xidian University, Xi'an, China

²Guangzhou Institute of Technology, Xidian University, Guangzhou, China

23171110703@stu.xidian.edu.cn, tengxiangyi@xidian.edu.cn, neouma@mail.xidian.edu.cn

Abstract

Multiplex graphs are widely used to model multi-relational complex systems and play an important role in various real-world scenarios such as financial systems and social networks. Hence, detecting anomalous samples in multiplex graph becomes crucial to ensure cybersecurity and stability. Although existing homogeneous graph anomaly detection (GAD) methods can be applied to deal with multiplex graphs, they still face two major challenges: 1) Due to the multiplicity and complexity of relations in multiplex graphs, homogeneous GAD models fail to effectively capture anomalous behaviors that correlate with diverse relational patterns. 2) In real-world applications, malicious entities usually disguise themselves through various camouflage strategies, making it difficult to capture subtle anomalous features via single-relation analysis. To address these challenges, we propose a novel unsupervised anomaly detection method for multiplex graphs based on **Similarity-constrained Fusion Graph Autoencoder** (SFGA). In SFGA, we design a multiplex graph autoencoder and introduced a cross-plex attention module at the model bottleneck to achieve comprehensive modeling of cross-relation anomaly patterns. Then, a similarity balancing strategy is proposed to constrain node representations at the bottleneck from both local and global perspectives, enhancing the discriminative power against camouflaged anomalies of autoencoder and enabling more effective identification of anomalous nodes with overlapping or deceptive patterns. Extensive experiments are conducted on both synthetic and real-world datasets at varying scales, and the results demonstrate our proposed method outperforms state-of-the-art approaches by a large margin.

Code — <https://github.com/zhaihuiliang/SFGA>

Extended version — [https://github.com/zhaihuiliang/SFGA_Fullversion_with_Appendix.pdf](https://github.com/zhaihuiliang/SFGA/SFGA_Fullversion_with_Appendix.pdf)

Introduction

Multiplex graph is a special type of heterogeneous graph (Shen, He, and Kang 2024) composed of shared node features and multiple relation graphs, where each subgraph

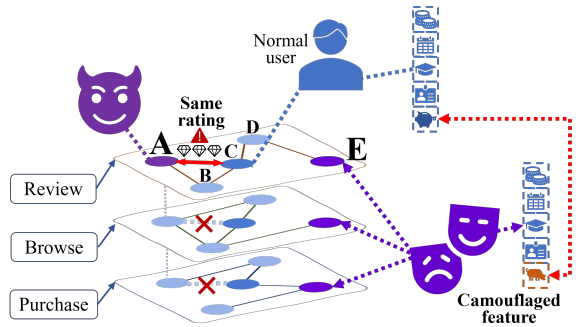


Figure 1: An example to demonstrate relation-specific anomalies (node A) and camouflaged anomalies (node E).

represents a specific type of relationship between nodes, enabling multi-dimensional modeling of complex node interactions. This powerful multi-relational representation capability makes it widely applicable across numerous scenarios such as social networks (Ma et al. 2021; Peng et al. 2023; Pan et al. 2025b), financial systems (Zhao et al. 2021; Wang et al. 2023), and e-commerce networks (Yang et al. 2022; Ni, Li, and McAuley 2019). To ensure the reliability and security of these real-world systems, it is crucial to perform anomaly detection on multiplex graphs, which enables the identification of abnormal samples that deviate from expected patterns. Taking e-commerce platform as an example, malicious users may fabricate fake reviews to boost product visibility (Liu et al. 2021c; Pan et al. 2025a) or distribute fraudulent links (Zhang et al. 2024a; Miao et al. 2025) to guide victims into fake websites. In this case, accurately identifying these anomalies is essential for maintaining a secure digital ecosystem and enhancing user experience.

Aiming to identify the abnormal samples in graph-structured data, graph anomaly detection (GAD) (Guo et al. 2023; Zhao et al. 2025) emerges as a potential solution to address this issue. Leveraging powerful unsupervised learning techniques, such as graph autoencoders (Ding et al. 2019) and graph contrastive learning (Liu et al. 2021b), existing GAD approaches are capable of detecting anomalies without requiring labeled instances, which greatly improves their applicability in real-world scenarios where annotated anomalies are scarce or unavailable. As the multi-relational inter-

*These authors contributed equally.

†Corresponding author.

actions can be collapsed into a homogeneous graph by treating all relation types uniformly, mainstream GAD methods can be potentially applied to detect anomalies in multiplex graphs.

While existing GAD methods for homogeneous graphs can be a feasible solution for anomaly detection in multiplex graphs, the unique characteristics of real-world multiplex graph data give rise to two major challenges that hinder their effectiveness. **Challenge 1 - relation-specific anomaly patterns.** Fraudulent behaviors may only manifest in one or several types of relation while performing normal in other types of relation, making it difficult for homogeneous GAD models to capture anomalies. For instance, in e-commerce review data (Dou et al. 2020a), a fraudulent user (e.g., node A in Fig. 1) may post suspiciously positive reviews for low-quality products (anomalous in the review graph) but show no corresponding activity in the browsing or purchase graphs. In this case, collapsing multiple relations into a homogeneous graph may eliminate important relational distinctions, making it harder to distinguish anomalous behavior from normal patterns. **Challenge 2 - camouflaged anomalies in multiplex graphs.** In real-world anomaly detection scenarios, malicious entities often employ various camouflage tactics to mimic the behaviors of normal users, making them hard to distinguish from benign ones (Zhang et al. 2024a; Dou et al. 2020a; Zhang et al. 2021). For example, fraudsters may post carefully timed reviews (Wen et al. 2020) or imitate common language styles (Dou et al. 2020b), causing their latent features to overlap with those of normal users (e.g., node E in Fig. 1). In the context of multiplex graphs, this challenge becomes more severe, since camouflaged anomalies can only be exposed by jointly analyzing behavioral consistency and topological signals in multiple relation types. As a result, directly applying homogeneous GAD methods may fail to capture subtle inconsistencies across relations, leading to reduced detection accuracy.

To address the above challenges, in this paper, we propose **Similarity-constrained Fusion Graph Autoencoder** (SFGA for short), a novel method specifically designed for unsupervised anomaly detection in multiplex graphs. To handle **Challenge 1**, we designed a multiplex graph autoencoder with inter-relation attention as the backbone model for anomaly detection of multiplex graphs. More specifically, the autoencoder conduct encoding and decoding based on each relational graph separately, which effectively captures and discriminates the relation-specific information. Meanwhile, a cross-plex attention module is employed at the autoencoder bottleneck to enable interactive information flow among multiple graphs, comprehensively modeling cross-relation patterns for anomaly detection. To overcome **Challenge 2**, we designed a similarity balancing strategy that constrains bottleneck node representations from both local and global perspectives, ensuring their distributions are well-regulated across multiple dimensions. The balancing strategy enhances the discriminative power of the autoencoder against camouflaged anomalies, making it more effective in identifying anomalies with overlapping or deceptive patterns in multiplex graphs. We conducted extensive experiments on four datasets with either real-world anom-

lies or injected anomalies, and the results show the superior anomaly detection capability of SFGA over state-of-the-art approaches.

Related Work

In this section, we briefly review two related research directions. A more detailed review is provided in Appendix A.

Multiplex graph learning. A multiplex graph is a graph composed of multiple views or multiple types of edges. Multiplex graph learning (MGL) aims to learn informative representations or make predictions from such graphs by considering both the structural and attributive information of different views. Based on whether label information is used for training, MGL approaches can be categorized into two categories: supervised (Yun et al. 2019; Zhang et al. 2019) and unsupervised methods (Park et al. 2020; Jing, Park, and Tong 2021). Representative supervised methods include (Hu et al. 2020; Wang et al. 2019b; Fu et al. 2020), whose approach is using graph neural networks (GNNs) (Kipf and Welling 2016; Velickovic et al. 2017; Hamilton, Ying, and Leskovec 2017) to project heterogeneous structures to homogeneous structures, which further trained by the supervision signals from label-guided downstream tasks. Due to the heavy costs of labels acquisition (Zhao et al. 2020), researchers pay more attention in unsupervised multiplex graph learning (UMGL). Pioneer studies on UMGL (Lin et al. 2021; Pan and Kang 2021) integrate graph filtering with spectral and subspace clustering to reveal underlying patterns in complex networks, while other UMGL methods (Liu et al. 2022b; Mo et al. 2023a; Qian, Li, and Kang 2024; Peng, Wang, and Zhu 2023; Mo et al. 2023b) adopt unsupervised approaches which utilizing GNNs to generate low-dimensional embeddings and leverage self-supervised learning for model optimization. The learned embeddings can be used in various downstream tasks, including node classification, clustering, and similarity search. However, existing methods mainly focus on representation learning but fail to apply to anomaly detection in multiplex graphs. Different from them, this paper aims to develop an end-to-end model to identify anomalous nodes from multiplex graphs.

Anomaly Detection on Graph. Graph anomaly detection (GAD) (Liu et al. 2021b) aims to identify nodes deviating statistically from the dominant pattern. Existing GAD methods comprise two categories: traditional and deep learning-based approaches (Pan et al. 2023). Traditional graph anomaly detection distinguishes outliers against normal nodes using non-deep learning methodologies (Perozzi and Akoglu 2016; Li et al. 2017; Peng et al. 2018; Wang et al. 2018; Huang et al. 2022). While traditional methods exhibit limited capacity for high-dimensional features and complex structures, deep learning-based GAD methods achieve higher precision and efficiency by effectively extracting hierarchical relational patterns. Deep learning-based methods primarily utilizes two techniques: generative learning and contrastive learning. Generative methods (Ding et al. 2019; Fan, Zhang, and Li 2020; Ding et al. 2021; Li et al. 2024) primarily employ GNNs as graph encoders to extract discriminative information within graphs.

Differently, contrastive learning-based methods detect graph anomalies by constructing multi-scale contrastive scenarios (Liu et al. 2021b; Jin et al. 2021; He et al. 2024; Huang et al. 2023; Zheng et al. 2021). Complementary to these two major paradigms, other GAD solutions (Zhou et al. 2021; Wang et al. 2021; Liu et al. 2022a) have also achieved promising results. However, most existing methods are designed for homogeneous edge relationships within single-layer graphs. In contrast, real-world scenarios often involve multiplex graphs with heterogeneous edges, posing significant challenges to identify anomalies from such graphs.

Preliminary

In this paper, we investigate unsupervised graph anomaly detection (GAD) problem on multiplex graphs due to the difficulty in acquiring labeled anomalies in complex real-world graphs. That is to say, the GAD models learn without both node category labels and anomaly labels. Specifically, the definition of multiplex graphs and the multiplex graph anomaly detection (MGAD) problem are given as follows.

Multiplex Graphs. Let $g = (\mathcal{V}, \mathbf{A}, \mathbf{X})$ denote a graph, where \mathcal{V} is its node set, \mathbf{A} is the adjacency matrix, and \mathbf{X} is the node features. A multiplex graph can be represented as $\mathcal{G} = \{g^{(1)}, g^{(2)}, \dots, g^{(R)}\}$, in which R denotes the number of graphs, $g^{(r)}$ denotes the r -th view in the multiplex graph. In $g^{(r)} = (\mathcal{V}, \mathbf{A}^{(r)}, \mathbf{X})$, $\mathbf{A}^{(r)}$ denotes the graph structure of each view, while \mathcal{V} and $\mathbf{X} \in \mathbb{R}^{N \times F}$ denote the set of all nodes and node features shared among all views, where $N = |\mathcal{V}|$ and F denote the number of nodes and size of node features, respectively.

MGAD Problem. Given a multiplex graph \mathcal{G} , the unsupervised MGAD problem aims to detect nodes that differ significantly from most others in terms of both structure and features. The objective is to learn an anomaly function $f(\cdot)$ to estimate the anomaly score of each node $v_i \in \mathcal{V}$, where a larger the score $f(v_i)$ indicates a higher probability of node v_i being anomalous.

Methodology

In this section, we introduce the proposed method, termed SFGA, designed for unsupervised anomaly detection in multiplex graphs. As illustrated in Figure 2, the backbone of the anomaly detection model is a *multiplex graph autoencoder*, where the discriminative knowledge from different relational graphs is encoded in separate channels of the autoencoder. To jointly capture inter-relational dependencies and enhance representation coherence, we further design an *attentive inter-relation fusion module* to fuse the bottleneck representations from different channels through a multi-view cross-attention mechanism, which facilitates the detection of subtle anomalies that only emerge through inconsistencies across multiple relation types. To detect camouflaged anomalies, we dedicately design a *similarity-constrained detection module* that enforces both neighbor-node similarity and far-node separability in the latent space, encouraging the model to amplify subtle deviations from typical node patterns even when features appear deceptively normal. Finally, a *hierarchical anomaly scoring module* is employed to

estimate the abnormality from both reconstruction error and local similarity. The following subsections provide detailed descriptions of each module.

Autoencoder with Attentive Inter-Relation Fusion

Relation Separated Autoencoder To identify anomalous samples from a homogeneous graph without supervision signals (i.e., labeled anomalies), a widely adopted solution is to build an autoencoder model as the basic detector (Ding et al. 2019; Fan, Zhang, and Li 2020; Zheng et al. 2021). Concretely, their key idea is to reconstruct the graph structure or node features from low-dimensional embeddings, under the assumption that anomalies will incur larger reconstruction errors due to their deviation from dominant patterns. Nevertheless, for multiplex graphs, it is crucial to consider the diverse interaction patterns across different relational graphs, as anomalies may only manifest in specific relations while remaining inconspicuous in others. In this case, a feasible solution is to encode each relational graph with separate autoencoder channels, which allows the model to preserve relation-specific structural and semantic patterns.

To this end, we first employ multiple channels of graph autoencoder with independent GCN layers to each relational graph. Specifically, for the r -th relational graph $g^{(r)}$, the corresponding encoder generates view-specific node representations $\mathbf{H}_i^{(r)}$ based on both node features and unique topological structures within each graph by:

$$\mathbf{H}_l^{(r)} = \sigma(\hat{\mathbf{D}}_r^{-\frac{1}{2}} \hat{\mathbf{A}}^{(r)} \hat{\mathbf{D}}_r^{-\frac{1}{2}} \mathbf{H}_{l-1}^{(r)} \mathbf{W}_l^{(r)}), \quad (1)$$

where $\hat{\mathbf{A}}^{(r)} = \mathbf{A}^{(r)} + w\mathbf{I}_N$, w indicates the weight of identity matrix, $\hat{\mathbf{D}}_r$ indicates the degree matrix of $\hat{\mathbf{A}}^{(r)}$, $\mathbf{W}_l^{(r)}$ indicates the trainable parameters, and $\sigma(\cdot)$ represents the non-linear activation function. Here, the input embedding $\mathbf{H}_0^{(r)} = \mathbf{X}$ is denoted as the raw feature, and the output, i.e., the bottleneck representations of autoencoder, is denoted as $\mathbf{H}^{(r)} = \mathbf{H}_L^{(r)}$, where L is the layer number. With such separate channel encoders, the bottleneck representations can effectively preserve the relation-specific structural and semantic knowledge, laying a solid foundation to capture relational anomaly patterns.

After encoding, the next step is to reconstruct the original data based on the low-dimensional bottleneck representations. Due to the overwhelming computational cost of reconstructing the full graph structure, in SFGA, we simplify the objective as only reconstructing the node features. Specifically, we attempt to use the learned latent representations $\mathbf{H}^{(r)}$ from each relational graph. In each channel, we predict the raw node features $\hat{\mathbf{X}}^{(r)}$ using a relation-specific MLP-based decoder, which can be written as follows:

$$\mathbf{H}'^{(r)} = \sigma(\mathbf{H}_{l-1}^{(r)} \mathbf{W}'^{(r)}), \quad (2)$$

where $\mathbf{W}'^{(r)}$ denotes the weight matrix of the l -th layer in the MLP, and $\sigma(\cdot)$ represents the non-linear activation function. In the decoder, the input is the bottleneck representation, i.e., $\mathbf{H}_0^{(r)} = \mathbf{H}^{(r)}$, and the final output is the reconstructed features, i.e., $\hat{\mathbf{X}}^{(r)} = \mathbf{H}_{L'}^{(r)}$.

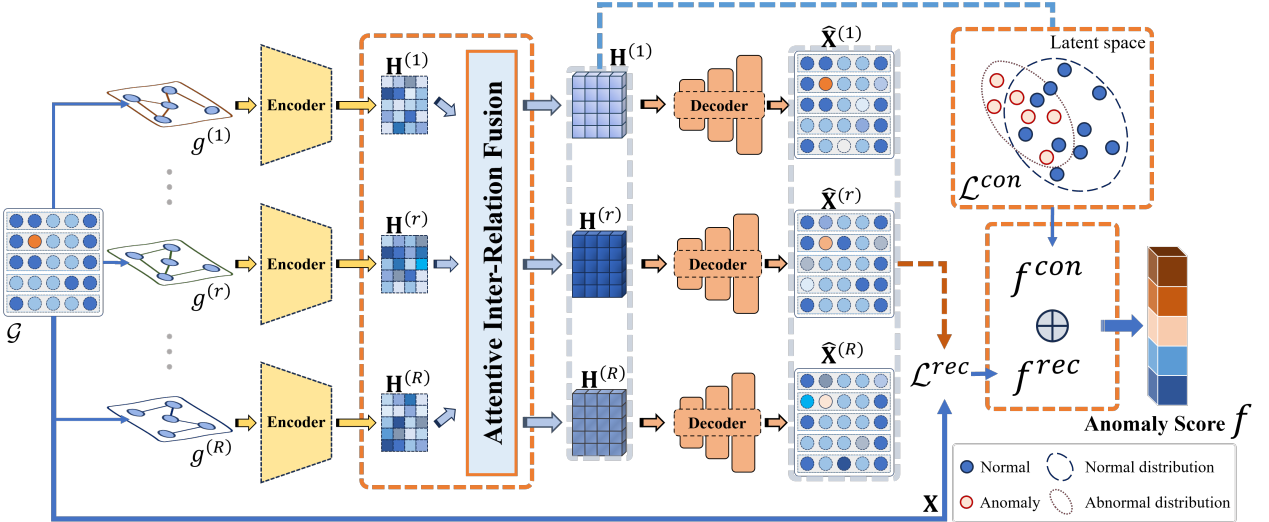


Figure 2: The overall pipeline of SFGA.

To optimize the graph autoencoder model, a reconstruction loss function is applied to minimize the reconstruction errors of node features, which can be represented by:

$$\mathcal{L}^{rec} = \frac{1}{N} \sum_{r=1}^R \sum_{i=1}^N (\hat{\mathbf{X}}^{(r)} - \mathbf{X})^2. \quad (3)$$

This term enforces that the reconstructed node features are closed to original input (i.e., the node features). In this way, the model learns to capture the dominant patterns of the multiplex graph data, while anomalies, which deviate significantly from these patterns, incur higher reconstruction errors and can thus be effectively detected.

Attentive Inter-Relation Fusion Although the relation-separated autoencoder allows the unique characteristics of each relational graph to be independently captured, it fails to model the interdependencies across different relations, which are often crucial for identifying cross-relation inconsistencies and subtle anomalies (Mo et al. 2023a; Jing, Park, and Tong 2021). To further enable information communication across different relational graphs, in SFGA, we design an attentive inter-relation fusion module that aggregates bottleneck representations from all relation-specific channels through a learnable cross-attention mechanism, which adaptively learns cross-relation information to capture complex abnormality in multiplex graphs.

Specifically, we designate the anchor view in the multiplex graph as the focal graph $g^{(f)}$, and the other graphs within the same multiplex graph as contextual graphs $g^{(c)}$ (here $f, c \in \{1, \dots, R\}$), then the representation importance of contextual graph $g^{(c)}$ for node i in focal graph $g^{(f)}$ can be calculated as:

$$\bar{\alpha}_i^{(c)} = \frac{1}{N} \sum_{m=1}^N \left(\mathbf{h}_i^{(f)} \mathbf{W}_q \right)^T \left(\mathbf{h}_m^{(c)} \mathbf{W}_k^{(c)} \right), \quad (4)$$

where $\bar{\alpha}_i^{(c)}$ denotes the importance of contextual graph c to

the representation of node i in the focal graph, $\mathbf{W}_k^{(c)}$ is the key transformation matrix specific to contextual graph c , $\mathbf{W}_q \in \mathbb{R}^{d \times d}$ is the query transformation matrix for node i in the focal graph, $\mathbf{h}_i^{(f)}$ represents the embedding of node i in the focal graph, $\mathbf{h}_m^{(c)}$ denotes the embedding of node m in contextual graph c , and N is the total number of nodes. We then obtain the weights of node representations from different views, i.e.,

$$\alpha_i^{(c)} = \frac{\exp(\bar{\alpha}_i^{(c)})}{\sum_{r=1}^R \exp(\bar{\alpha}_i^{(r)})}, \quad (5)$$

where $\alpha_i^{(c)}$ represents the importance weight of the c -th contextual graph for node i in the focal graph. The final fused representation $\tilde{\mathbf{h}}_i^{(f)}$ of node i is obtained through weighted aggregation:

$$\tilde{\mathbf{h}}_i^{(f)} = \sum_{r=1}^R \alpha_i^{(r)} \mathbf{h}_i^{(r)}. \quad (6)$$

By concatenating the fused representations of all nodes, the fused representation matrix $\mathbf{H}^{(f)}$ can be used for downstream decoder and further processing. This attentive fusion mechanism enables the model to selectively integrate complementary signals across relational views, which enhances its capacity to detect complex, relation-inconsistent anomalies that are otherwise overlooked in isolated views.

Similarity-Constrained Detection Module

While the graph autoencoder-based backbone effectively captures dominant structural and attribute patterns, it may suffer from insufficient discriminability when faced with camouflaged anomalies or overlapping node representations (Li et al. 2024). In multiplex graphs, the situation can be more severe since camouflaged anomalies may exhibit normal behavior in most relation types, making them difficult to distinguish (Zhang et al. 2024a). To uncover cam-

ouflaged anomalies, an effective approach is to leverage local similarity patterns (Li et al. 2024; Qiao and Pang 2023). More specifically, although these anomalies mimic normal node features, such feature-level camouflage can disrupt the inherent homophily property of the graph, which causes the latent representation of an abnormal node to deviate significantly from those of its neighbors.

Building on this intuition, in SFGA, we employ a homophily-aware similarity balancing strategy that guides model training through both local and global distributional constraints in latent space, ultimately optimizing feature representations and also forming a powerful detection module. To be more specific, within each view of the multiplex graph structure, we enhance the average similarity between node representations and their 1-hop neighbor representations in latent space, forcing the model to focus on latent relationships between adjacent node pairs. The similarity can be:

$$sim_{i|\text{nei}}^{(r)} = \frac{1}{N_{i|\text{nei}}^{(r)}} \sum_{j=1}^{N_{i|\text{nei}}^{(r)}} \frac{\tilde{\mathbf{h}}_i^{(r)\top} \tilde{\mathbf{h}}_j^{(r)}}{\|\tilde{\mathbf{h}}_i^{(r)}\| \cdot \|\tilde{\mathbf{h}}_j^{(r)}\|}, \quad (7)$$

where $sim_{i|\text{nei}}^{(r)}$ denotes the average representation similarity between node i and its 1-hop neighbors in the r -th view, where $\tilde{\mathbf{h}}_j^{(r)} \in \{\tilde{\mathbf{h}}_j^{(r)} | v_j \in \mathcal{N}_i^{(r)}\}$, $\mathcal{N}_i^{(r)}$ represents the 1-hop neighborhood set of node v_i , and $N_{i|\text{nei}}^{(r)}$ indicates the cardinality of node v_i 's 1-hop neighborhood set.

Simultaneously, we reduce the average similarity between node representations and their non-1-hop neighbors in latent space, forcing the model to learn a more reasonable global node representation distribution:

$$sim_{i|\text{global}}^{(r)} = \frac{1}{N_{i|\text{dis}}^{(r)}} \sum_{k=1}^{N_{i|\text{dis}}^{(r)}} \frac{\tilde{\mathbf{h}}_i^{(r)\top} \tilde{\mathbf{h}}_k^{(r)}}{\|\tilde{\mathbf{h}}_i^{(r)}\| \|\tilde{\mathbf{h}}_k^{(r)}\|}, \quad (8)$$

here, $sim_{i|\text{global}}^{(r)}$ denotes the average representation similarity between node i and its non-1-hop neighbors in the r -th view, where $\tilde{\mathbf{h}}_k^{(r)} \in \{\tilde{\mathbf{h}}_k^{(r)} | v_k \notin \mathcal{N}_i^{(r)}\}$, and $N_{i|\text{dis}}^{(r)}$ indicates the number of disconnected nodes from v_i in view r .

To maximize the local similarity while minimizing the global one, the constraint loss for the i -th node is given as:

$$\mathcal{L}^{con} = \sum_{v_i \in \mathcal{V}} \sum_{r=1}^R (sim_{i|\text{global}}^{(r)} - sim_{i|\text{nei}}^{(r)}). \quad (9)$$

This constraint encourages the model to learn locally coherent yet globally discriminative node representations, making camouflaged anomalies more distinguishable from their neighbors. Importantly, it complements the autoencoder-based backbone by injecting structure-aware supervision into the latent space, and the local similarity can also serve as an indicator of node abnormality.

To jointly optimize node attribute reconstruction errors and representation constraint errors, the objective function of our model can be formulated as:

$$\mathcal{L} = \alpha \mathcal{L}^{rec} + (1 - \alpha) \mathcal{L}^{con}, \quad (10)$$

where α is a controlling parameter which balances the impacts of reconstruction and similarity constraint.

Hierarchical Anomaly Scoring

After sufficient training iterations, anomalies hidden within nodes start to manifest progressively. As the loss function (Eq. (9)) optimizing, a subset of anomalous nodes are initially detected during the representation constraint phase. That is to say, nodes that fail to exhibit normal local similarity patterns are more likely to be identified as anomalies. We begin by evaluating node abnormality from this perspective as following:

$$f(v_i)^{con} = - \sum_{r=1}^R \frac{1}{N_{i|\text{nei}}^{(r)}} \sum_{j=1}^{N_{i|\text{nei}}^{(r)}} \frac{\tilde{\mathbf{h}}_i^{(r)\top} \tilde{\mathbf{h}}_j^{(r)}}{\|\tilde{\mathbf{h}}_i^{(r)}\| \cdot \|\tilde{\mathbf{h}}_j^{(r)}\|}. \quad (11)$$

At the same time, the reconstruction errors can also indicate the abnormality of nodes. Hence, we can compute the anomaly score of each node v_i according to:

$$f(v_i)^{rec} = \sum_{r=1}^R \|\hat{\mathbf{x}}_i^{(r)} - \mathbf{x}_i\|_2. \quad (12)$$

Finally, the node anomaly score in the multiplex graph is the summation of the scores from the two phases:

$$f(v_i) = \beta f(v_i)^{rec} + (1 - \beta) f(v_i)^{con}, \quad (13)$$

where β is a controlling parameter to balance the the scores of different levels. The overall algorithm of our SFGA is proposed in Appendix B, with the time complexity of $O(r \cdot N^2 \cdot h)$ and detailed complexity analysis is given in Appendix C.

Experiments

Experimental Setup

Datasets. To ensure sufficient coverage of different experimental data types, we conducted experiments on two small-scale datasets with manually injected synthetic anomalies: IMDB (Wang et al. 2019b) and Freebase (Mo et al. 2023b), one medium-sized and one large real-world dataset containing fraudulent anomalies: Amazon-fraud and YelpChi-fraud (Dou et al. 2020a). We injected two types of anomalies into originally normal datasets: contextual anomalies created by swapping node attributes, and structural anomalies generated by disrupting node connections. When injecting both types, we maintained equal quantities for each, following prior research (Ding et al. 2019; Liu et al. 2024). The specific details of anomaly injection and the statistics of datasets are presented in Appendix D.

Baselines. We employ three categories of unsupervised GAD methods as baselines: 1) methods based on contrastive learning including **CoLA** (Liu et al. 2021b), **PREM** (Pan et al. 2023) and **AD-GCL** (Xu et al. 2025), 2) methods based on graph autoencoders including **DOMINANT** (Ding et al. 2019), **ADA-GAD** (He et al. 2024) and **GADAM** (Chen et al. 2024), and 3) method based on message passing represented by **TAM** (Qiao and Pang 2023). A summary of the

| Method | IMDB(I) | | | Freebase(I) | | Amazon(R) | | YelpChi(R) | |
|-------------|-------------------|-------------------|-------------------|--------------------|-------------------|--------------------|-------------------|-------------------|--|
| | AUROC | AUPRC | AUROC | AUPRC | AUROC | AUPRC | AUROC | AUPRC | |
| TAM | 70.38±1.24 | 26.64±4.31 | 84.89±3.74 | 38.88±2.97 | 71.13±6.56 | 34.19±12.47 | OOM | OOM | |
| CoLA | 56.01±0.49 | 9.14±0.18 | 55.38±0.54 | 6.55±0.19 | 25.01±0.20 | 5.05±0.05 | 54.25±0.05 | 16.38±0.04 | |
| PREM | 65.20±0.49 | 14.31±0.30 | 53.26±0.74 | 6.46±0.32 | 68.42±4.62 | 22.27±7.45 | 49.96±5.01 | 15.07±2.34 | |
| DOMINANT | 75.19±0.59 | 24.38±1.87 | 60.14±0.53 | 11.73±0.58 | 49.54±3.69 | 6.16±0.28 | 48.92±0.40 | 14.85±0.30 | |
| ADA-GAD | 58.11±0.01 | 10.39±0.08 | 54.54±0.10 | 6.29±0.03 | 26.23±0.04 | 4.25±0.01 | 47.07±0.01 | 13.96±0.01 | |
| GADAM | 71.41±0.08 | 19.82±0.37 | 75.81±2.72 | 19.44±1.37 | 51.83±0.60 | 7.18±0.19 | 51.28±0.27 | 14.80±0.10 | |
| AD-GCL | 64.33±0.93 | 15.24±1.31 | 64.05±1.42 | 9.10±0.79 | 28.15±1.04 | 4.83±0.18 | OOM | OOM | |
| SFGA | 80.33±0.37 | 43.07±0.37 | 92.98±2.84 | 58.50±12.10 | 78.48±3.06 | 16.39±1.80 | 70.06±0.33 | 24.68±0.40 | |

Table 1: Results in terms of AUROC and AUPRC (in percent \pm standard deviation) on 4 datasets, with **the best results** highlighted in bold black, where “I” indicates datasets with injected anomalies and “R” indicates which with real anomalies. OOM indicates Out-Of-Memory on a 96GB GPU.

| Component | | | Amazon | | YelpChi | |
|-----------|----|----|-------------------|-------------------|-------------------|-------------------|
| ATT | SC | HD | AUROC | AUPRC | AUROC | AUPRC |
| - | - | - | 71.86±7.77 | 13.76±3.78 | 51.44±1.07 | 15.68±0.47 |
| - | ✓ | ✓ | 73.13±0.57 | 15.64±0.77 | 59.63±1.44 | 19.83±1.17 |
| ✓ | - | ✓ | 73.47±4.48 | 13.17±2.53 | 67.99±0.81 | 22.43±0.28 |
| ✓ | ✓ | - | 77.69±2.74 | 15.79±1.85 | 67.82±0.65 | 22.33±0.25 |
| ✓ | ✓ | ✓ | 78.48±3.06 | 16.39±1.80 | 70.06±0.33 | 24.68±0.40 |

Table 2: Ablation study results on Amazon and YelpChi of SFGA, with **the best results** highlighted in bold black.

baselines are provided in Appendix E. Moreover, to ensure a relatively more fair comparison and apply these GAD methods initially designed for homogeneous graphs to multiplex graphs, we treat all edges in the multiplex graph as a single edge type, thereby collapsing them into homogeneous graphs, the specific processing procedures are presented in Appendix D.

Evaluation Metrics. Consistent with established graph anomaly detection research (Liu et al. 2021b; Ding et al. 2019), we measure the performance on all these methods using two evaluation metrics: AUROC (Area Under the Receiver Operating Curve) and AUPRC (Area Under the Precision-Recall Curve).

Experimental details. To ensure fair comparison, we conducted moderate parameter tuning for all baseline methods to maximize their performance. For our proposed SFGA, we employ a single-layer GCN as the encoder for the r -th view, where the embedding dimension is set to D_E . As the dataset scales differ, we set different numbers of linear layers L for the MLP-based decoder, configure different quantities of hidden units, and correspondingly adjust the learning rate based on the specific dataset scales. Additionally, all parameters are optimized with the Adam optimizer (Kingma 2014) using the same weight decay, and we use ReLU (Nair and Hinton 2010) function as the nonlinear activation function. To ensure consistency, all methods report the average results from 10 independent runs for comparison. The implementation details and architectural configurations of our method during experiments are shown in Appendix F.

Experimental Results

Performance Comparison. According to the results presented in Table 1, we have the below analysis based on these observations. 1) Although we have conducted parameter tuning for all baselines to maximize their performance potential on multiplex graphs, our proposed SFGA still demonstrates superior performance compared to these baselines. Specifically, on the Freebase and Amazon datasets, SFGA achieves approximately 8% higher AUROC than the second-best method in the group. Moreover, in terms of the AUPRC, SFGA demonstrates over 16% improvement compared to the best baseline results on both the IMDB and Freebase datasets. This validates the effectiveness of our proposed method while demonstrating that such GAD methods initially designed for homogeneous graphs are not suitable for multiplex graphs. 2) On the IMDB dataset, the reconstruction-based DOMINANT outperforms other baselines, yet still shows a 5% gap in AUROC compared to SFGA. This demonstrates that the representation constraint mechanism effectively improves node embeddings in the latent space and mitigates distribution overlapping. 3) On the YelpChi dataset, all baselines exhibit suboptimal detection performance compared to SFGA, which indicates the application potential of SFGA in large-scale datasets. In summary, with the exploitation of inter-relation correlations and constraints on node embeddings in latent space, SFGA can capture more task-relevant information, thereby enhancing its anomaly detection performance.

Ablation Study. To validate the effectiveness of key components in SFGA, we conducted ablation studies on multiple variants of the complete SFGA framework, with all results shown in Table 2. Here, ATT, SC, and HD denote the inter-relation attention mechanism, similarity-based constraint mechanism, and hierarchical anomaly detector in our proposed method, respectively.

Through analysis of the obtained results, we draw the following conclusions: 1) Compared with the variant without ATT, our proposed SFGA demonstrates significant improvements in both metrics, exemplified by 10-percentage-point and 5-percentage-point increases in AUROC and AUPRC respectively on the YelpChi dataset. This indicates

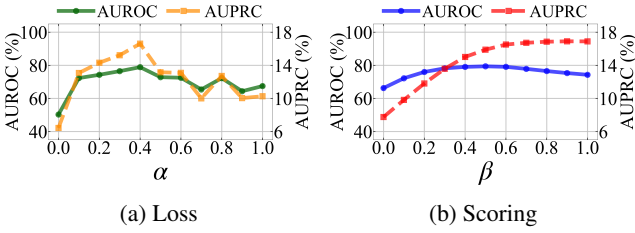


Figure 3: The effect of the trade-off parameters α and β on loss and scoring.

that the inter-relation attention mechanism can integrate complementary signals from multiple relations, yielding substantial impact on downstream anomaly detection tasks. 2) In contrast to the variant without **SC**, SFGA also performs better in both metrics, indicating that the similarity-based constraint mechanism plays a critical role in optimizing the representation quality of the model and enhancing its discriminative capability for camouflaged anomalies. 3) The contribution of **HD** remains non-negligible, as it can expand the anomaly detection scope of the model to enhance its performance. Finally, compared to the variant devoid of **ATT**, **SC**, and **HD**, our method demonstrates substantial superiority across all metrics. This indicates that the proposed inter-relation attention mechanism, similarity-based constraint mechanism, and hierarchical anomaly detector can effectively collaborate during training to mutually enhance the anomaly detection performance of SFGA.

Parameter Analysis. To investigate how parameters α in Eq. (10) and β in Eq. (13) affect performance under different settings, we specifically tested anomaly detection on the Amazon-fraud dataset. We varied the parameter values from 0 to 1 with stride = 0.1 and present the results in Figure 3.

As shown in Fig. 3a, we observe that variations in α , which controls the weighting between the reconstruction loss and representation constraint loss terms, lead to corresponding fluctuations in both AUROC and AUPRC performance metrics, and both evaluation metrics get the best when α approaches 0.4. However, performance becomes unstable when the representation constraint loss weight falls below 0.5. Notably, extreme α values (approaching either 1 or 0) consistently lead to degraded model performance. From these we can observe that the weight ratio between the two loss terms significantly impacts model performance, while also revealing that the representation constraint mechanism effectively reduces feature overlap caused by ‘camouflage’ in fraud data, evidenced by the performance fluctuations when α exceeds 0.5.

Fig. 3b reveals that the AUROC metric goes to top when β approaches 0.5, then declines as β nears extreme values (0 or 1). In contrast, AUPRC shows a gradual improvement with increasing β values, reaching its maximum when $\beta \geq 0.8$. This proves the feature reconstruction detector in SFGA, with the balancing strategy, can effectively identify attribute anomalies with camouflage characteristics, but relying too much on it limits detection performance, which proves again the effectiveness of our hierarchical anomaly

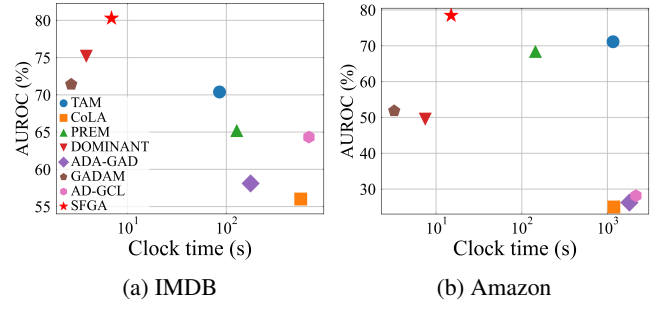


Figure 4: Efficiency comparison based on training time required to achieve optimal results.

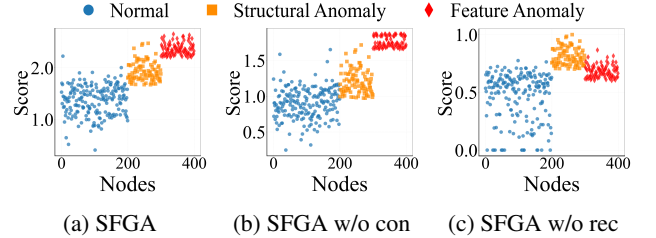


Figure 5: Visualization results on IMDB dataset.

detection mechanism.

Efficiency Analysis. To further verify the efficiency of SFGA, we compare the training time required to achieve optimal results with baseline methods on IMDB and Amazon datasets. For the training of all methods, we fixed the model parameters that yielded the results reported in Table 1, the total time cost and corresponding detection results are presented in Fig. 4a and 4b. The results demonstrate that while SFGA ranks 3rd across both datasets in terms of computational cost, its attainment of best performance validates comprehensive superiority over all baselines.

Visualization. We further visualize the anomaly score distributions learned by different components of our method on the IMDB dataset in Fig. 5. As shown in Fig. 5a, we observe a clear stratification between anomaly scores of normal and abnormal nodes learned by SFGA, where the combination of the two detectors creates distinct separation between feature anomalies and structural anomalies. When using only the feature reconstruction detector for anomaly detection, Fig. 5b clearly shows that the detected feature-anomalous nodes have significantly higher anomaly scores than structural-anomalous nodes, proving our feature anomaly detector works as intended. Correspondingly, when using only the similarity-based constraint detector for anomaly detection, Fig. 5c demonstrates that structural-anomalous nodes achieve significantly higher anomaly scores than feature-anomalous nodes while maintaining clear separation from normal nodes, which confirms the strong effectiveness of such detector in identifying structural anomalies. In summary, such clear anomaly score boundaries demonstrate the outstanding detection capability of our proposed method.

Conclusion

In this paper, we proposed SFGA, a novel unsupervised multiplex graph anomaly detection method. Through an inter-relation attentive module and a carefully-designed representation balancing mechanism, SFGA generates high-quality node representations and further produces highly discriminative reconstructed features, ultimately achieving effective graph anomaly detection on multiplex graphs by jointly considering both feature reconstruction errors and similarity-based constraints. Extensive experiments reveal the effectiveness and superior of our proposed method.

In future work, we plan to further optimize the computational efficiency of SFGA to extend its application to very large-scale multiplex graphs, and investigate the possibility integrated with large language model for a more accurate anomaly detection.

Acknowledgments

This work was supported in part by the National Natural Science Foundation of China under Grants 62306224 and 62471371, in part by the Guangdong High-level Innovation Research Institution Project under Grant 2021B0909050008, and in part by the Guangzhou Key Research and Development Program under Grant 202206030003.

References

- Chen, J.; Zhu, G.; Yuan, C.; and Huang, Y. 2024. Boosting graph anomaly detection with adaptive message passing. In *The 12th International Conference on Learning Representations*.
- Ding, K.; Li, J.; Agarwal, N.; and Liu, H. 2021. Inductive anomaly detection on attributed networks. In *Proceedings of the 29th International Conference on International Joint Conferences on Artificial Intelligence*, 1288–1294.
- Ding, K.; Li, J.; Bhanushali, R.; and Liu, H. 2019. Deep anomaly detection on attributed networks. In *Proceedings of the 2019 SIAM International Conference on Data Mining*, 594–602. SIAM.
- Dou, Y.; Liu, Z.; Sun, L.; Deng, Y.; Peng, H.; and Yu, P. S. 2020a. Enhancing graph neural network-based fraud detectors against camouflaged fraudsters. In *Proceedings of the 29th ACM International Conference on Information & Knowledge Management*, 315–324.
- Dou, Y.; Ma, G.; Yu, P. S.; and Xie, S. 2020b. Robust spammer detection by nash reinforcement learning. In *Proceedings of the 26th ACM SIGKDD International Conference on Knowledge Discovery & Data Mining*, 924–933.
- Fan, H.; Zhang, F.; and Li, Z. 2020. Anomalydae: Dual autoencoder for anomaly detection on attributed networks. In *ICASSP 2020-2020 IEEE International Conference on Acoustics, Speech and Signal Processing*, 5685–5689. IEEE.
- Fan, S.; Wang, X.; Shi, C.; Lu, E.; Lin, K.; and Wang, B. 2020. One2multi graph autoencoder for multi-view graph clustering. In *Proceedings of the Web Conference*, 3070–3076.
- Fu, X.; Zhang, J.; Meng, Z.; and King, I. 2020. Magnn: Metapath aggregated graph neural network for heterogeneous graph embedding. In *Proceedings of the Web Conference*, 2331–2341.
- Guo, J.; Tang, S.; Li, J.; Pan, K.; and Wu, L. 2023. Rustgraph: Robust anomaly detection in dynamic graphs by jointly learning structural-temporal dependency. *IEEE Transactions on Knowledge and Data Engineering*, 36(7): 3472–3485.
- Hamilton, W.; Ying, Z.; and Leskovec, J. 2017. Inductive representation learning on large graphs. volume 30.
- He, J.; Xu, Q.; Jiang, Y.; Wang, Z.; and Huang, Q. 2024. Ada-gad: Anomaly-denoised autoencoders for graph anomaly detection. In *Proceedings of the AAAI Conference on Artificial Intelligence*, volume 38, 8481–8489.
- Hu, Z.; Dong, Y.; Wang, K.; and Sun, Y. 2020. Heterogeneous graph transformer. In *Proceedings of the Web Conference*, 2704–2710.
- Huang, T.; Pei, Y.; Menkovski, V.; and Pechenizkiy, M. 2022. Hop-count based self-supervised anomaly detection on attributed networks. In *Joint European Conference on Machine Learning and Knowledge Discovery in Databases*, 225–241. Springer.
- Huang, Y.; Wang, L.; Zhang, F.; and Lin, X. 2023. Unsupervised graph outlier detection: Problem revisit, new insight, and superior method. In *2023 IEEE 39th International Conference on Data Engineering*, 2565–2578. IEEE.
- Jin, M.; Liu, Y.; Zheng, Y.; Chi, L.; Li, Y.-F.; and Pan, S. 2021. Anemone: Graph anomaly detection with multi-scale contrastive learning. In *Proceedings of the 30th ACM International Conference on Information & Knowledge Management*, 3122–3126.
- Jing, B.; Park, C.; and Tong, H. 2021. Hdmi: High-order deep multiplex infomax. In *Proceedings of the Web Conference*, 2414–2424.
- Khoshraftar, S.; and An, A. 2024. A survey on graph representation learning methods. *ACM Transactions on Intelligent Systems and Technology*, 15(1): 1–55.
- Kingma, D. P. 2014. Adam: A method for stochastic optimization. *arXiv preprint arXiv:1412.6980*.
- Kipf, T. N.; and Welling, M. 2016. Semi-supervised classification with graph convolutional networks. *arXiv preprint arXiv:1609.02907*.
- Li, J.; Dani, H.; Hu, X.; and Liu, H. 2017. Radar: Residual analysis for anomaly detection in attributed networks. In *IJCAI*, volume 17, 2152–2158.
- Li, J.; Gao, Y.; Lu, J.; Fang, J.; Wen, C.; Lin, H.; and Wang, X. 2024. DiffGAD: A Diffusion-based Unsupervised Graph Anomaly Detector. *arXiv preprint arXiv:2410.06549*.
- Li, X.; Li, Y.; Mo, X.; Xiao, H.; Shen, Y.; and Chen, L. 2023. Diga: Guided diffusion model for graph recovery in anti-money laundering. In *Proceedings of the 29th ACM SIGKDD Conference on Knowledge Discovery and Data Mining*, 4404–4413.

- Lin, Z.; Kang, Z.; Zhang, L.; and Tian, L. 2021. Multi-view attributed graph clustering. *IEEE Transactions on Knowledge and Data Engineering*, 35(2): 1872–1880.
- Liu, F.; Ma, X.; Wu, J.; Yang, J.; Xue, S.; Beheshti, A.; Zhou, C.; Peng, H.; Sheng, Q. Z.; and Aggarwal, C. C. 2022a. Dadag: Data augmentation for graph anomaly detection. In *2022 IEEE International Conference on Data Mining*, 259–268. IEEE.
- Liu, K.; Dou, Y.; Ding, X.; Hu, X.; Zhang, R.; Peng, H.; Sun, L.; and Yu, P. S. 2024. Pygod: A python library for graph outlier detection. *Journal of Machine Learning Research*, 25(141): 1–9.
- Liu, K.; Zhang, H.; Hu, Z.; Wang, F.; and Yu, P. S. 2023. Data augmentation for supervised graph outlier detection with latent diffusion models. *arXiv preprint arXiv:2312.17679*.
- Liu, L.; Kang, Z.; Ruan, J.; and He, X. 2022b. Multilayer graph contrastive clustering network. *Information Sciences*, 613: 256–267.
- Liu, X.; Zhang, F.; Hou, Z.; Mian, L.; Wang, Z.; Zhang, J.; and Tang, J. 2021a. Self-supervised learning: Generative or contrastive. *IEEE Transactions on Knowledge and Data Engineering*, 35(1): 857–876.
- Liu, Y.; Li, Z.; Pan, S.; Gong, C.; Zhou, C.; and Karypis, G. 2021b. Anomaly detection on attributed networks via contrastive self-supervised learning. *IEEE Transactions on Neural Networks and Learning Systems*, 33(6): 2378–2392.
- Liu, Y.; Pan, S.; Wang, Y. G.; Xiong, F.; Wang, L.; Chen, Q.; and Lee, V. C. 2021c. Anomaly detection in dynamic graphs via transformer. *IEEE Transactions on Knowledge and Data Engineering*, 35(12): 12081–12094.
- Ma, X.; Wu, J.; Xue, S.; Yang, J.; Zhou, C.; Sheng, Q. Z.; Xiong, H.; and Akoglu, L. 2021. A comprehensive survey on graph anomaly detection with deep learning. *IEEE Transactions on Knowledge and Data Engineering*, 35(12): 12012–12038.
- Miao, R.; Liu, Y.; Wang, Y.; Shen, X.; Tan, Y.; Dai, Y.; Pan, S.; and Wang, X. 2025. Blindguard: Safeguarding llm-based multi-agent systems under unknown attacks. *arXiv preprint arXiv:2508.08127*.
- Mo, Y.; Chen, Y.; Lei, Y.; Peng, L.; Shi, X.; Yuan, C.; and Zhu, X. 2023a. Multiplex graph representation learning via dual correlation reduction. *IEEE Transactions on Knowledge and Data Engineering*, 35(12): 12814–12827.
- Mo, Y.; Lei, Y.; Shen, J.; Shi, X.; Shen, H. T.; and Zhu, X. 2023b. Disentangled multiplex graph representation learning. In *International Conference on Machine Learning*, 24983–25005. PMLR.
- Nair, V.; and Hinton, G. E. 2010. Rectified linear units improve restricted boltzmann machines. In *Proceedings of the 27th International Conference on Machine Learning (ICML-10)*, 807–814.
- Ni, J.; Li, J.; and McAuley, J. 2019. Justifying recommendations using distantly-labeled reviews and fine-grained aspects. In *Proceedings of the 2019 Conference on Empirical Methods in Natural Language Processing and the 9th International Joint Conference on Natural Language Processing*, 188–197.
- Pan, E.; and Kang, Z. 2021. Multi-view contrastive graph clustering. *Advances in Neural Information Processing Systems*, 34: 2148–2159.
- Pan, E.; and Kang, Z. 2023. High-order multi-view clustering for generic data. *Information Fusion*, 100: 101947.
- Pan, J.; Liu, Y.; Zheng, X.; Zheng, Y.; Liew, A. W.-C.; Li, F.; and Pan, S. 2025a. A label-free heterophily-guided approach for unsupervised graph fraud detection. In *Proceedings of the AAAI Conference on Artificial Intelligence*, volume 39, 12443–12451.
- Pan, J.; Liu, Y.; Zheng, Y.; and Pan, S. 2023. Prem: A simple yet effective approach for node-level graph anomaly detection. In *2023 IEEE International Conference on Data Mining*, 1253–1258. IEEE.
- Pan, J.; Zheng, Y.; Tan, Y.; and Liu, Y. 2025b. A Survey of Generalization of Graph Anomaly Detection: From Transfer Learning to Foundation Models. *arXiv preprint arXiv:2509.06609*.
- Park, C.; Kim, D.; Han, J.; and Yu, H. 2020. Unsupervised attributed multiplex network embedding. In *Proceedings of the AAAI Conference on Artificial Intelligence*, volume 34, 5371–5378.
- Peng, L.; Mo, Y.; Xu, J.; Shen, J.; Shi, X.; Li, X.; Shen, H. T.; and Zhu, X. 2023. GRLC: Graph representation learning with constraints. *IEEE Transactions on Neural Networks and Learning Systems*.
- Peng, L.; Wang, X.; and Zhu, X. 2023. Unsupervised multiplex graph learning with complementary and consistent information. In *Proceedings of the 31st ACM International Conference on Multimedia*, 454–462.
- Peng, Z.; Luo, M.; Li, J.; Liu, H.; Zheng, Q.; et al. 2018. ANOMALOUS: A Joint Modeling Approach for Anomaly Detection on Attributed Networks. In *IJCAI*, volume 18, 3513–3519.
- Perozzi, B.; and Akoglu, L. 2016. Scalable anomaly ranking of attributed neighborhoods. In *Proceedings of the 2016 SIAM International Conference on Data Mining*, 207–215. SIAM.
- Qian, X.; Li, B.; and Kang, Z. 2024. Upper bounding barlow twins: A novel filter for multi-relational clustering. In *Proceedings of the AAAI Conference on Artificial Intelligence*, volume 38, 14660–14668.
- Qiao, H.; and Pang, G. 2023. Truncated affinity maximization: One-class homophily modeling for graph anomaly detection. *Advances in Neural Information Processing Systems*, 36: 49490–49512.
- Sadikaj, Y.; Rass, J.; Velaj, Y.; and Plant, C. 2023. Semi-supervised embedding of attributed multiplex networks. In *Proceedings of the ACM Web Conference*, 578–587.
- Shen, Z.; He, H.; and Kang, Z. 2024. Balanced multi-relational graph clustering. In *Proceedings of the 32nd ACM International Conference on Multimedia*, 4120–4128.

- Velickovic, P.; Cucurull, G.; Casanova, A.; Romero, A.; Lio, P.; Bengio, Y.; et al. 2017. Graph attention networks. volume 1050, 10–48550.
- Wang, D.; Lin, J.; Cui, P.; Jia, Q.; Wang, Z.; Fang, Y.; Yu, Q.; Zhou, J.; Yang, S.; and Qi, Y. 2019a. A semi-supervised graph attentive network for financial fraud detection. In *2019 IEEE International Conference on Data Mining*, 598–607. IEEE.
- Wang, H.; Zhou, C.; Wu, J.; Dang, W.; Zhu, X.; and Wang, J. 2018. Deep structure learning for fraud detection. In *2018 IEEE International Conference on Data Mining*, 567–576. IEEE.
- Wang, X.; Ji, H.; Shi, C.; Wang, B.; Ye, Y.; Cui, P.; and Yu, P. S. 2019b. Heterogeneous graph attention network. In *the World Wide Web Conference*, 2022–2032.
- Wang, X.; Jin, B.; Du, Y.; Cui, P.; Tan, Y.; and Yang, Y. 2021. One-class graph neural networks for anomaly detection in attributed networks. *Neural Computing and Applications*, 33: 12073–12085.
- Wang, Y.; Zhang, J.; Huang, Z.; Li, W.; Feng, S.; Ma, Z.; Sun, Y.; Yu, D.; Dong, F.; Jin, J.; et al. 2023. Label information enhanced fraud detection against low homophily in graphs. In *Proceedings of the ACM Web Conference*, 406–416.
- Wen, R.; Wang, J.; Wu, C.; and Xiong, J. 2020. Asa: Adversary situation awareness via heterogeneous graph convolutional networks. In *Companion Proceedings of the Web Conference*, 674–678.
- Xu, Y.; Peng, Z.; Shi, B.; Hua, X.; Dong, B.; Wang, S.; and Chen, C. 2025. Revisiting Graph Contrastive Learning on Anomaly Detection: A Structural Imbalance Perspective. In *Proceedings of the AAAI Conference on Artificial Intelligence*, volume 39, 12972–12980.
- Yang, Y.; Huang, C.; Xia, L.; Liang, Y.; Yu, Y.; and Li, C. 2022. Multi-behavior hypergraph-enhanced transformer for sequential recommendation. In *Proceedings of the 28th ACM SIGKDD Conference on Knowledge Discovery and Data Mining*, 2263–2274.
- Yuan, X.; Zhou, N.; Yu, S.; Huang, H.; Chen, Z.; and Xia, F. 2021. Higher-order structure based anomaly detection on attributed networks. In *2021 IEEE International Conference on Big Data*, 2691–2700. IEEE.
- Yun, S.; Jeong, M.; Kim, R.; Kang, J.; and Kim, H. J. 2019. Graph transformer networks. In *Advances in Neural Information Processing Systems*, volume 32.
- Zhang, C.; Song, D.; Huang, C.; Swami, A.; and Chawla, N. V. 2019. Heterogeneous graph neural network. In *Proceedings of the 25th ACM SIGKDD International Conference on Knowledge Discovery & Data Mining*, 793–803.
- Zhang, G.; Wu, J.; Yang, J.; Beheshti, A.; Xue, S.; Zhou, C.; and Sheng, Q. Z. 2021. Fraudre: Fraud detection dual-resistant to graph inconsistency and imbalance. In *2021 IEEE International Conference on Data Mining*, 867–876. IEEE.
- Zhang, J.; Xu, Z.; Lv, D.; Shi, Z.; Shen, D.; Jin, J.; and Dong, F. 2024a. DiG-In-GNN: discriminative feature guided GNN-based fraud detector against inconsistencies in multi-relation fraud graph. In *Proceedings of the AAAI Conference on Artificial Intelligence*, volume 38, 9323–9331.
- Zhang, Y.; Ma, X.; Wu, J.; Yang, J.; and Fan, H. 2024b. Heterogeneous subgraph transformer for fake news detection. In *Proceedings of the ACM Web Conference*, 1272–1282.
- Zhao, J.; Wang, X.; Shi, C.; Liu, Z.; and Ye, Y. 2020. Network schema preserving heterogeneous information network embedding. In *International Joint Conference on Artificial Intelligence*.
- Zhao, K.; Zhang, Z.; Rong, Y.; Yu, J. X.; and Huang, J. 2021. Finding critical users in social communities via graph convolutions. *IEEE Transactions on Knowledge and Data Engineering*, 35(1): 456–468.
- Zhao, Y.; Liu, Y.; Li, S.; Chen, Q.; Zheng, Y.; and Pan, S. 2025. Freeгад: A training-free yet effective approach for graph anomaly detection. *arXiv preprint arXiv:2508.10594*.
- Zheng, X.; Wu, B.; Liang, X.; and Li, W. 2024. Friend or foe? Mining suspicious behavior via graph capsule infomax detector against fraudsters. In *Proceedings of the ACM Web Conference*, 2684–2693.
- Zheng, Y.; Jin, M.; Liu, Y.; Chi, L.; Phan, K. T.; and Chen, Y.-P. P. 2021. Generative and contrastive self-supervised learning for graph anomaly detection. *IEEE Transactions on Knowledge and Data Engineering*, 35(12): 12220–12233.
- Zhou, S.; Tan, Q.; Xu, Z.; Huang, X.; and Chung, F.-l. 2021. Subtractive aggregation for attributed network anomaly detection. In *Proceedings of the 30th ACM International Conference on Information & Knowledge Management*, 3672–3676.
- Zhuo, W.; Liu, Z.; Hooi, B.; He, B.; Tan, G.; Fathony, R.; and Chen, J. 2024. Partitioning message passing for graph fraud detection. *arXiv preprint arXiv:2412.00020*.

Appendix

A. Related Work in Detail

We first review the recent development of unsupervised multiplex graph learning. After that, we summarize recent advances in different anomaly detection methods for graphs.

Unsupervised Multiplex Graph Learning (UMGL). Unlike supervised approaches (Yun et al. 2019; Zhang et al. 2019; Hu et al. 2020; Wang et al. 2019b; Fu et al. 2020; Sadikaj et al. 2023), unsupervised multiplex graph learning (UMGL) addresses unsupervised tasks in multiplex graphs by leveraging both node features and graph structures (Pan and Kang 2023). In exploratory approaches within the UMGL direction, representative works such as **MvAGC** (Lin et al. 2021) and **MCGC** (Pan and Kang 2021) primarily attempt to uncover latent structural patterns in complex networks by integrating graph filtering with unsupervised learning techniques, including spectral clustering and subspace clustering.

With the advancement of deep representation learning (Khoshrftar and An 2024), researchers have integrated graph neural networks (GNNs) (Kipf and Welling 2016; Velickovic et al. 2017; Hamilton, Ying, and Leskovec 2017) with self-supervised techniques (Liu et al. 2021a) to develop UMGL methods for learning node representations, and applied the obtained representations to downstream tasks such as node classification. Additionally, **O2MAC** (Fan et al. 2020) first attempted to apply GNNs in UMGL model, this method pioneers a deep one-to-multi graph autoencoder framework for attributed multi-view graph clustering, resolving dual challenges of multi-view fusion and clustering-oriented embedding through unified optimization. Some researchers also fuse the representations of different relations by maximizing the mutual information between local and global contexts. **DMGI** (Park et al. 2020) innovatively implements an unsupervised consensus regularization framework for attributed multiplex networks, resolving representation conflicts across relation types through universal discriminators and attention-based fusion. **HDMI** (Jing, Park, and Tong 2021) proposes a high-order mutual information framework that jointly optimizes the interdependencies between node embeddings and global summaries (extrinsic signals) as well as node embeddings and attributes (intrinsic signals), while designing an attention fusion module to integrate multi-relational layer embeddings, achieving unsupervised multi-view network representation learning.

Among these efforts, some works achieve coordinated optimization and alignment of relational representations by employing multiple contrastive loss functions, while effectively preventing dimensional collapse. **MGCCN** (Liu et al. 2022b) proposes an unsupervised multi-layer graph contrastive clustering framework that captures node-neighbor relationships through an attention-based GCN encoder (self-reconstruction), aligns heterogeneous information via cross-layer contrastive learning, and iteratively refines embeddings and cluster centers with a dynamic centroid alignment strategy, achieving end-to-end joint optimization of three key objectives: topological reconstruction, cross-layer consistency, and discriminative cluster structure. **MGDCR** (Mo

et al. 2023a) proposes a multi-layer graph dual-correlation reduction framework that jointly optimizes intra-layer denoising and inter-layer alignment, achieving self-supervised multi-layer graph representation learning without negative samples. **BTGF** (Qian, Li, and Kang 2024) proposes a Barlow Twins-bounded graph filter that theoretically proves the positive semi-definite inner product of input features can provide a loss upper bound, and designs a feature-structure doubly-constrained filter to achieve multi-relational graph clustering. Another line of work adopts the approach of jointly learning inter-graph consistency and complementary features to achieve comprehensive representation learning of multi-graph information. **CoCoMG** (Peng, Wang, and Zhu 2023) proposes a dual-constrained multi-graph learning framework that extracts complementary information through an MLP encoder and captures consistent information via canonical correlation analysis, addressing out-of-sample inference and noise robustness challenges in multi-graph learning. **DMG** (Mo et al. 2023b) proposes a multi-graph decoupled representation learning framework that achieves graph information decoupling and fusion through a cross-graph commonality alignment loss and an intra-graph private information purification loss.

However, despite significant progress, the application of current UMGL methods to anomaly detection in multiplex graphs remains an overlooked research area, and our method aims to develop an end-to-end approach for identifying anomalous nodes in multiplex graphs.

Anomaly Detection on Graph. In graph anomaly detection (GAD), some researchers have achieved promising results by employing GNNs in semi-supervised anomaly detection approaches (Wang et al. 2019a; Zhang et al. 2024b). Specially, **CapsGI** (Zheng et al. 2024) proposes a capsule graph information maximization framework that decouples node capsules to extract intrinsic attributes while reinforcing normal node associations through capsule graph contrastive learning, addressing the behavior-label inconsistency problem in anomaly detection. **PMP** (Zhuo et al. 2024) proposes a partitioning message passing framework that addresses label imbalance and the homophily-heterophily mixture problem in fraud detection through label-aware neighbor partitioning aggregation and node-adaptive weight generation.

Due to the frequent lack of data labels in real-world applications, GAD research has predominantly focused on unsupervised methods, gradually advancing toward medium- and large-scale datasets. The generative learning method typically utilizes reconstruction error for anomaly detection. **Dominant** (Ding et al. 2019) proposes a graph convolutional autoencoder framework that achieves unsupervised graph anomaly detection through a dual-channel reconstruction mechanism for both structure and attributes, where the anomaly score is calculated as the reconstruction error. **AnomalyDAE** (Fan, Zhang, and Li 2020) proposes a dual-channel autoencoder framework that jointly captures complex relationships between network structure and node attributes through dual-path reconstruction and cross-modal interaction mechanisms, achieving high-precision anomaly detection. **AEGIS** (Ding et al. 2021) proposes an inductive graph anomaly detection framework that captures anomaly-

aware representations through graph meta-layers and enhances model generalization via adversarial generative training, enabling incremental anomaly detection without re-training. **GUIDE** (Yuan et al. 2021) proposes a higher-order structure-aware dual autoencoder framework that jointly captures anomalous behaviors in node attributes and topological patterns through network motif-based modeling of higher-order interactions and structural difference attention mechanisms. **VGOD** (Huang et al. 2023) proposes a variance-based dual-model framework that jointly optimizes a structural anomaly detection model and an attribute reconstruction model to address data leakage and detection imbalance issues in graph anomaly detection.

Contrastive learning-based methods detect graph anomalies based on the loss obtained from contrastive learning. **SL-GAD** (Zheng et al. 2021) proposes a context-subgraph-based self-supervised framework that achieves unsupervised graph anomaly detection through collaborative synergy between generative attribute reconstruction and multi-view contrastive learning modules. **AD-GCL** (Xu et al. 2025) proposes a structure-imbalance-aware graph contrastive learning framework that addresses the detection bottleneck for low-degree tail nodes through differentiated head/tail node augmentation strategies and dual-view consistency constraints, achieving robust anomaly detection. **CoLA** (Liu et al. 2021b) proposes a target node-local subgraph contrastive learning framework that achieves unsupervised attributed graph anomaly detection through multi-round neighbor subgraph sampling and a dual-channel discrimination mechanism. **Anemone** (Jin et al. 2021) proposes a multi-scale contrastive learning framework that achieves attributed graph anomaly detection through dual-granularity contrast at node-level and neighborhood-level, combined with a statistical anomaly estimator. **ADA-GAD** (He et al. 2024) proposes a two-stage anomaly-denoising autoencoder framework that addresses the anomaly overfitting and homophily trap issues in graph anomaly detection through multi-level graph augmentation pretraining and node anomaly distribution regularization.

Additionally, researchers have approached anomaly detection from a spatial distance perspective, distinguishing anomalous nodes based on differences in spatial distances. **AAGNN** (Zhou et al. 2021) proposes a neighbor-deviation-based anomaly detection framework that achieves unsupervised graph anomaly detection through subtractive aggregation characterizing node abnormality and hypersphere learning objectives. **OCGNN** (Wang et al. 2021) proposes a one-class graph neural network framework that drives GNNs to learn compact representations of normal nodes through hypersphere learning objectives, achieving topology-aware graph anomaly detection. **PREM** (Pan et al. 2023) proposes a preprocess-match dual-module framework that achieves efficient graph anomaly detection without training-time message passing through anonymized message passing for neighbor feature precomputation and a lightweight self-neighbor matching network.

In recent years, researchers have integrated diffusion models into GAD tasks, proposing numerous promising methods. **Diga** (Li et al. 2023) proposes a guided diffusion

model-based subgraph recovery framework that achieves high-precision graph anomaly detection in anti-money laundering scenarios through a three-stage process of biased subgraph sampling, conditional graph diffusion and weight-sharing GNN. **GODM** (Liu et al. 2023) introduces a latent diffusion model-powered graph anomaly data augmentation framework, which synthesizes high-fidelity anomalous nodes via sequential heterogeneous information encoding, latent space diffusion, and conditional graph generation operations, effectively mitigating class imbalance challenges. **DiffGAD** (Li et al. 2024) introduces a latent diffusion-powered discriminative content distillation framework for unsupervised graph anomaly detection, employing a cascaded architecture that sequentially performs generic content preservation, shared feature construction and discriminative content separation.

However, when existing methods encounter multiplex graphs with heterogeneous edges in real-world scenarios, their performance often falls short of expectations, which once again poses challenges for research in this field.

B. Summary of SFGA

The computational process of SFGA is summarized in Algorithm 1. As we can see, during each iteration, we initially train the multiplex graph autoencoder using both the reconstruction loss \mathcal{L}^{rec} and constraint loss \mathcal{L}^{con} for e_i steps. During this stage, the multiplex graph autoencoder first reconstructs node original features using their fused representations across different layers, while \mathcal{L}^{rec} enforces the reconstructed node features to be closed to original input. Additionally, \mathcal{L}^{con} optimizes the node representations in latent space by maximizing similarity between connected node pairs while minimizing similarity between unconnected node pairs. Through this approach, the reconstruction loss \mathcal{L}^{rec} and similarity constraint loss \mathcal{L}^{con} mutually enhance each other's effectiveness. Then, $f(v_i)^{rec}$ identifies a subset of anomalous nodes through feature reconstruction errors, while $f(v_i)^{con}$ detects anomalies based on deviations in the constrained similarity. Finally, SFGA computes each node's anomaly score by fusing $f(v_i)^{rec}$ and $f(v_i)^{con}$.

C. Complexity Analysis

In this section, we briefly analyze the time complexity of each component in SFGA. The time complexity of the relation separated autoencoder is $O(r \cdot (N^2 \cdot h + N \cdot h \cdot c + L \cdot N \cdot h^2))$, where N is the number of nodes, d is the original node feature dimension, h is the hidden layer dimension, c is the encoder representation dimension, and r is the number of layers in the multiplex graph, L is the number of decoder layers. For the attentive inter-relation fusion mechanism, the time complexity is $O(r \cdot N^2 \cdot c)$. Since h and c are of the same order, the time complexity of the multiplex graph autoencoder can be simplified to $O(r \cdot N^2 \cdot h)$. For the feature reconstruction loss \mathcal{L}_{rec} , the time complexity is $O(r \cdot N \cdot d)$, while both the local and global terms of the similarity constraint loss have a time complexity of $O(r \cdot N^2 \cdot c)$. Since d and c are of the same order, the overall computational complexity of the model's loss function is $O(r \cdot N^2 \cdot c)$.

Algorithm 1: Our proposed SFGA

Input: Node original attributes \mathbf{X} and the graph structures $\mathbf{A}^{(r)}$ of each layer in multiplex graph \mathcal{G} for $\forall r \in [1, R]$.
Parameter: Non-negative parameters α and β , number of outer iterations e_o , number of inner iterations e_i , learning rate of relation separated autoencoder l_r .
Output: The anomaly scores of each node in \mathcal{G} .

- 1: Randomly initialize the parameters of all modules of this method.
- 2: **for** $outer_iter = 1$ to e_o **do**
- 3: **for** $inner_iter = 1$ to e_i **do**
- 4: Obtain view-specific nodes representations $\mathbf{H}^{(r)}$ by Eq. (1).
- 5: Obtain the fused representations $\mathbf{H}^{(f)}$ by Eq. (6).
- 6: Reconstruct $\hat{\mathbf{X}}^{(r)}$ by decoding $\mathbf{H}^{(r)}$ by Eq. (2).
- 7: Calculate losses:
- 8: \mathcal{L}^{rec} between $\hat{\mathbf{X}}^{(r)}$ and \mathbf{X} by Eq. (3).
- 9: $sim_{i|nei}^{(r)}$ for (v_i, v_j) pairs by Eq. (7).
- 10: $sim_{i|global}^{(r)}$ for (v_i, v_k) pairs by Eq. (8).
- 11: constraint loss \mathcal{L}^{con} by Eq. (9).
- 12: objective function \mathcal{L} by Eq. (10).
- 13: Backpropagate \mathcal{L} to update parameters.
- 14: **end for**
- 15: **end for**
- 16: Calculate anomaly scores $f(v_i)^{con}$ of constraint loss by Eq. (11).
- 17: Calculate anomaly scores $f(v_i)^{rec}$ based on reconstruction errors by Eq. (12).
- 18: Calculate the final anomaly scores $f(v_i)$ of nodes by Eq. (13).

Correspondingly, The complexity of feature reconstruction anomaly scoring $f(v_i)^{con}$ is $O(r \cdot N \cdot d)$, while the anomaly scoring of similarity constraint $f(v_i)^{rec}$ is $O(r \cdot N^2 \cdot c)$. To sum up, the time complexity of our proposed method can be expressed as $O(r \cdot N^2 \cdot h + L \cdot N \cdot h^2 + r \cdot N^2 \cdot c + r \cdot N \cdot d)$. Since $L \ll N, d, c$, and h are of the same order, the overall time complexity of our proposed method can be simplified to $O(r \cdot N^2 \cdot h)$.

D. Datasets Description

We perform anomaly detection experiments on four public multiplex graph datasets of varying scales across different domains, including two movie-domain multiplex graphs (Mo et al. 2023b) IMDB and Freebase with injected anomalies, along with two real-world e-commerce fraud datasets (Dou et al. 2020a; Zhang et al. 2024a) Amazon-fraud and YelpChi-fraud containing genuine anomalies.

Details of Synthetic Anomaly Injection. Specifically, the anomalies injected into IMDB and Freebase include both structural anomalies and attribute anomalies, where attribute anomalies are introduced following the prior work (Liu et al. 2021b). We use a different approach to inject structural anomalies: place n fully-connected cliques (each containing m nodes) within randomly selected subgraphs. That is

to say, when placing each fully-connected clique, we first randomly select a subgraph from the multiplex graph, then choose m nodes within it to form complete connections, and exclude already marked anomalous nodes in subsequent operations. This process repeats n times, ultimately generating $m \times n$ structurally anomalous nodes in the multiplex graph.

Details of Collapsing Multiplex Graph into Homogeneous Graph. After obtaining the multiplex graph containing anomalies, we first perform element-wise summation of the adjacency matrices from all subgraphs to generate a fused matrix. Subsequently, we binarize the fused matrix by setting connections with values ≥ 1 to 1 while preserving others as 0, ultimately obtaining a multi-layer fused adjacency matrix. Through the aforementioned steps, we collapse the anomalous multiplex graph into an anomalous homogeneous graph.

Table 3 shows the data statistics including the number of nodes, edges, the dimension of the features, and the anomalies rate of the datasets, other details are described as follows:

- **IMDB** A relational movie network where nodes represent individual films categorized into three genres (action, comedy, drama), containing 4,780 movies in total. Its subgraphs correspond to two meta-paths: movie-actor-movie (MAM) and movie-director-movie (MDM). Features of each movie are generated from plot summaries using a bag-of-words (BoW) model, resulting in 1,232-dimensional vectors.
- **Freebase** A movie relationship dataset comprises three relation types: movie-actor-movie (MAM), movie-director-movie (MDM), and movie-writer-movie (MWM). It contains 3,492 films categorized into four genres (action, comedy, drama, documentary). Since the original dataset lacks raw features, we follow prior work (Mo et al. 2023b) to implement one-hot encoding for all node (movie) features.
- **Amazon-fraud** A dataset originates from the Amazon e-commerce platform, where nodes represent platform users containing activity data of 11,944 users. It encodes user-user interactions through three distinct adjacency matrices: user-product-user (UPU), user-star-user (USU), and user-text-user (UVU). Specifically, UPU connects users who have reviewed at least one common product, USU links users who gave identical star ratings within a one-week window, and UVU associates users with linguistically similar review styles.
- **YelpChi-fraud** A dataset derived from lodging and restaurant review data on Yelp, where all reviews are categorized as either spam or legitimate. This dataset comprises 45,954 reviews and constructs three subgraphs based on distinct inter-review relationships: review-user-review (RUR), review-time-review (RTR), and review-StarRate-review (RSR). Here, RUR connects reviews posted by the same user, RTR links reviews published within identical time windows, and RSR associates reviews sharing the same star ratings.

| Datasets | Nodes | Edges | Scale | Anomaly(I/R) | Ratio(%) | Relationships | Features |
|---------------|--------|-----------------------------------|--------|--------------|----------|---|----------------|
| IMDB | 4,780 | 98,110 21,018 | Small | 400(I) | 8.37 | Movie-Actor-Movie (MAM) Movie-Director-Movie (MDM) | 1,232 (BoW) |
| Freebase | 3,492 | 254,702 8,404 10,706 | Small | 200(I) | 5.73 | Movie-Actor-Movie (MAM) Movie-Director-Movie (MDM) Movie-Writer-Movie (MWM) | 3492 (one-hot) |
| Amazon-fraud | 11,944 | 175,608 3,566,479 1,036,737 | Medium | 821(R) | 6.87 | User-Product-User (UPU) User-Star rate-User (USU) User-Text-User (UVU) | 25 (handcraft) |
| YelpChi-fraud | 45,954 | 49,315 573,616 3,402,743 | Large | 6674(R) | 14.52 | Review-User-Review (RUR) Review-Time-Review (RTR) Review-Star rate-Review (RSR) | 32 (handcraft) |

Table 3: Statistics of all datasets.

| Settings | IMDB | Freebase | Amazon-fraud | YelpChi-fraud |
|--------------|------|----------|--------------|---------------|
| e_o | 10 | 10 | 10 | 2 |
| e_i | 10 | 10 | 10 | 10 |
| Hidden units | 128 | 128 | 128 | 512 |
| D_E | 128 | 8 | 8 | 64 |
| l_r | 1e-4 | 1e-3 | 1e-2 | 1e-4 |
| L | 2 | 3 | 3 | 4 |
| α | 0.9 | 0.4 | 0.4 | 0.9 |
| β | 0.5 | 0.3 | 0.7 | 0.2 |
| Weight decay | 1e-4 | 1e-4 | 1e-4 | 1e-4 |
| w | 1 | 1 | 1 | 1 |
| Dropout | 0.1 | 0.1 | 0.1 | 0.1 |

Table 4: Settings for the proposed SFGA.

E. Baselines Details

We adopt the following anomaly detection methods as baselines:

- **TAM** (Qiao and Pang 2023): This approach detects anomalies by enhancing local node proximity through affinity-driven representation learning and selectively pruning heterophilous connections to eliminate structural noise.
- **CoLA** (Liu et al. 2021b): This approach detects anomalies by contrasting node-subgraph compatibility through self-supervised representation learning, leveraging multi-round sampling to quantify local structural deviations.
- **PREM** (Pan et al. 2023): This approach detects anomalies by decoupling feature preprocessing from ego-neighbor matching, which not only removes message-passing operations during training but also measures structural compatibility using anonymized similarity metrics.
- **DOMINANT** (Ding et al. 2019): This approach detects anomalies by jointly reconstructing graph topology and nodes attributes through graph convolutional autoencoders, then quantify the abnormality of nodes via structural and attribute reconstruction errors.
- **ADA-GAD** (He et al. 2024): This approach detects anomalies by first pretraining on graphs with denoised anomaly signals, then refining the anomaly score distributions. Such dual-phase approach prevents overfitting

to spurious anomaly patterns through spectral-based data augmentation and entropy-driven regularization.

- **GADAM** (Chen et al. 2024): This approach introduces a neighborhood heterogeneity quantification framework that decouples interference from GNN signal propagation and amplifies anomaly discernment through context-aware message modulation.
- **AD-GCL** (Xu et al. 2025): This approach introduces a structural imbalance-aware framework that resolves performance disparity in tail anomaly detection and enhances robustness through dual adaptive neighborhood modulation.

F. Implementation Details

Hyperparameters. We performed a focused grid search on key hyperparameters that significantly impact model performance, while keeping less sensitive hyperparameters at fixed values (e.g., weight decay, self-connection weight w and dropout). The optimal hyperparameters obtained for each experimental dataset are presented in Table 4, with the grid search conducted within the following parameter space:

- Number of outer training iterations e_o : {2, 3, 5, 10, 15}
- Number of inner training iterations e_i : {5, 10, 15}
- Hidden units number of encoders: {16, 64, 128, 256, 512}
- Dimensions of node embeddings D_E : {8, 16, 64, 128}
- Learning rate of encoders l_r : {1e-4, 5e-4, 1e-3, 5e-3, 1e-2}
- Layer number of decoders L : {2, 3, 4, 5}
- Controlling parameter of objective function α : $\alpha \in [0, 1]$ with stride = 0.1
- Controlling parameter of anomaly scoring function β : $\beta \in [0, 1]$ with stride = 0.1

Computing environment. We implement the proposed SFGA with the following libraries: Python 3.9.21, PyTorch 1.21.1, CUDA_version 11.3, PyTorch_geometric 2.3.1 and Networkx 3.1.

Hardware configuration. For small and medium-scale datasets (e.g., IMDB, Freebase and Amazon-fraud), our experiments were conducted on a server equipped with one

NVIDIA RTX 3090 GPU and one Intel i7-10700K CPU. For the large-scale dataset (e.g., YelpChi-fraud), we used a server with one H20-NVLink GPU (96GB memory) and one Intel Xeon Platinum 8457C CPU.